

Analytical model of the enhanced light transmission through subwavelength metal slits: Green's function formalism versus Rayleigh's expansion

S. V. Kukhlevsky^a, M. Mechler^b, O. Samek^c, K. Janssens^d

^a*Institute of Physics, University of Pécs,
Ifjúság u. 6, Pécs 7624, Hungary*

^b*South-Trans-Danubian Cooperative Research Centre,
University of Pécs, Ifjúság u. 6, Pécs 7624, Hungary*

^c*Institute of Spectrochemistry and Applied Spectroscopy,
Bunsen-Kirchhoff-Str. 11, D-44139 Dortmund,
Germany*

^d*Department of Chemistry,
University of Antwerp, Universiteitsplein 1,
B-2610 Antwerp, Belgium*

We present an analytical model of the resonantly enhanced transmission of light through a subwavelength nm-size slit in a thick metal film. The simple formulae for the transmitted electromagnetic fields and the transmission coefficient are derived by using the thin-slit approximation and the Green function formalism for the solution of Maxwell's equations. The resonance wavelengths are in agreement with the semi-analytical model [Y. Takakura, Phys. Rev. Lett. **86**, 5601 (2001)], which solves the wave equations by using the Rayleigh field expansion. Our formulae, however, show great resonant enhancement of a transmitted wave, while the Rayleigh expansion model predicts attenuation. The difference is attributed to the near-field subwavelength diffraction, which is not considered by the models based on the Rayleigh expansion.

PACS numbers: 78.66.Bz, 42.25.Fx, 07.79.Fc, 42.79.Ag

I. INTRODUCTION

The near-field localization and resonantly enhanced transmission of light by metal subwavelength nanostructures, such as a single aperture, a grating of apertures or an aperture surrounded by grooves, attract increasing interest of researchers. The recent studies^{1,2,3,4,5,6,7,8,9,10} have pointed out that the localization and enhanced (anomalous) transmission of light by a grating of holes or slits can be better understood by elucidating the optical properties of a single subwavelength slit. Along this direction, it was already demonstrated that a TM-polarized light wave can be localized in the near-field subwavelength zone of a metal slit and simultaneously enhanced by a factor of about 10-10^{32,3,4,5,6,7,8,9,10,11,12,13}. The general analysis and interpretation of these results, however, are very complicated because the studies are based mainly on purely numerical computer models. Recently, a simple semi-analytical model of the light transmission by a subwavelength metal slit was developed¹. The study clearly showed that the transmission coefficient versus wavelength possesses a Fabry-Perot-like resonant behavior. Unfortunately, the model¹ predicts transmission peaks with very low magnitude (attenuation), while the experiments and computer models^{2,3,4,5,6,7,8,9,10} demonstrate the great resonant enhancement of a transmitted wave.

In this paper, we present an analytical model of the resonantly enhanced transmission of light through a subwavelength nm-size metal slit. The simple formulae for the transmitted electromagnetic fields and the transmission coefficient are derived by using the thin-slit approximation and the Green function formalism for the solution of Maxwell's equations. The article is organized as follows. The model and formulae are described in section II. In section III, the model is compared with the results of the semi-analytical model¹. We show that the resonance wavelengths determined by our formulae are in agreement with the model¹, which solves the wave equations by using the Rayleigh field expansion. The formulae, however, indicate great resonant enhancement of a transmitted wave, while the Rayleigh expansion model¹ predicts attenuation. The summary and conclusion are given in section IV.

II. ANALYTICAL MODEL BASED ON GREEN'S FUNCTION FORMALISM

a. Theoretical background Let us consider the scattering of TM-polarized light by a subwavelength slit in a thick metallic film of perfect conductivity. From the latter metal property it follows that surface plasmons do not exist in the film. Such a metal is described by the classic Drude model for which the plasmon frequency tends towards infinity. We follow the Neerhoff and Mur theoretical development based on the Green function formalism for the solution of Maxwell's equations^{11,12,13}.

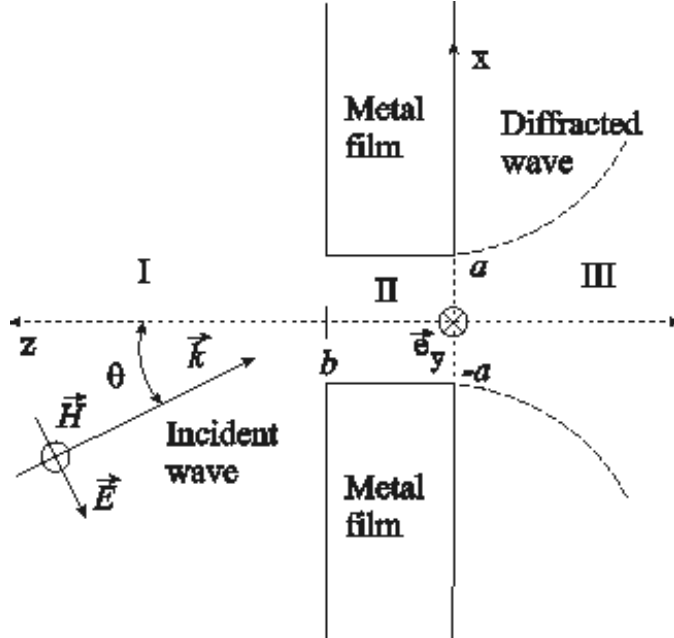


FIG. 1: Schematic diagram of light scattering by a subwavelength slit (waveguide) in a thick metallic film.

The schematic diagram of the light scattering is shown in Fig. 1. The transmission of a plane wave through a subwavelength ($\lambda < 2a$) slit of width $2a$ in a metal film of thickness b is considered. In region I, the incident wave propagates in the $(x - z)$ plane at an angle Θ with respect to the z axis. The magnetic field of the wave is assumed to be time harmonic with the frequency $\omega = kc$ and both polarized and constant in the y direction:

$$\vec{H}(x, y, z, t) = U(x, z)\exp(-i\omega t)\vec{e}_y. \quad (1)$$

The electric field of the wave is found from the scalar field $U(x, z)$ using Maxwell's equations. Thus, the electromagnetic field is determined by a single scalar field $U(x, z)$. In the regions I, II and III, the field is represented by $U_1(x, z)$, $U_2(x, z)$ and $U_3(x, z)$, respectively. The field satisfies the Helmholtz equation $(\nabla^2 + k_j^2)U_j = 0$, where $j = 1, 2, 3$. In region I, the field $U_1(x, z)$ is decomposed into three components, $U_1(x, z) = U^i(x, z) + U^r(x, z) + U^d(x, z)$, each of which satisfies the Helmholtz equation. The incident field $U^i(x, z) = \exp[ik_1(x \sin \Theta - z \cos \Theta)]$ is assumed to be a plane wave of unit amplitude. $U^r(x, z) = U^i(x, 2b - z)$ denotes the field that would be reflected if there were no slit in the film. U^d describes the field diffracted by the slit into region I. To find the field, the 2-dimensional Green's theorem is applied with one function given by $U(x, z)$ and the other by a conventional Green's function:

$$(\nabla^2 + k_j^2)G_j = -\delta(x - x', z - z'), \quad (2)$$

where (x, z) refers to a field point of interest; x' and z' are integration variables, $j = 1, 2, 3$. Since U_j satisfies the Helmholtz equation, Green's theorem reduces to

$$U(x, z) = \int_{\text{Boundary}} (G\partial_n U - U\partial_n G)dS. \quad (3)$$

The unknown fields $U^d(x, z)$, $U_3(x, z)$ and $U_2(x, z)$ respectively for the regions ($b < z < \infty$), ($-\infty < z < 0$) and ($|x| < a, 0 < z < b$) are found using the reduced Green's theorem and the standard boundary conditions for a perfectly conducting film

$$U^d(x, z) = -\frac{\epsilon_1}{\epsilon_2} \int_{-a}^a G_1(x, z; x', b) D U_b(x') dx', \quad (4)$$

$$U_3(x, z) = \frac{\epsilon_3}{\epsilon_2} \int_{-a}^a G_3(x, z; x', 0) D U_0(x') dx', \quad (5)$$

$$U_2(x, z) = - \int_{-a}^a [G_2(x, z; x', 0) DU_0(x') - U_0(x') \partial_{z'} G_2(x, z; x', z')|_{z \rightarrow 0+}] dx' \\ + \int_{-a}^a [G_2(x, z; x', b) DU_b(x') - U_b(x') \partial_{z'} G_2(x, z; x', z')|_{z \rightarrow b-}] dx'. \quad (6)$$

The boundary fields are defined from the continuity of the tangential components of \vec{H} and \vec{E} :

$$U_0(x) = U_2(x, z)|_{z \rightarrow 0+}, \quad (7)$$

$$DU_0(x) = \partial_z U_2(x, z)|_{z \rightarrow 0+}, \quad (8)$$

$$U_b(x) = U_2(x, z)|_{z \rightarrow b-}, \quad (9)$$

$$DU_b(x) = \partial_z U_2(x, z)|_{z \rightarrow b-}. \quad (10)$$

In regions I and III the Green's functions are given by

$$G_1(x, z; x', z') = \frac{i}{4} [H_0^{(1)}(k_1 R) + H_0^{(1)}(k_1 R')], \quad (11)$$

$$G_3(x, z; x', z') = \frac{i}{4} [H_0^{(1)}(k_3 R) + H_0^{(1)}(k_3 R'')], \quad (12)$$

with $R = [(x - x')^2 + (z - z')^2]^{1/2}$, $R' = [(x - x')^2 + (z + z' - 2b)^2]^{1/2}$ and $R'' = [(x - x')^2 + (z + z')^2]^{1/2}$. Here, $H_0^{(1)}$ is the Hankel function. Inside the waveguide (region II), the method of images can be used; the Green's function is given by the waveguide multimode ($m = \infty$) expansion

$$G_2(x, z; x', z') = \frac{i}{4a\gamma_0} \exp(i\gamma_0|z - z'|) + \frac{i}{2a} \sum_{m=1}^{\infty} \gamma_m^{-1} \\ \times \cos[m\pi(x + a)/2a] \cos[m\pi(x' + a)/2a] \\ \times \exp(i\gamma_m|z - z'|), \quad (13)$$

where $\gamma_m = [k_2^2 - (m\pi/2a)^2]^{1/2}$. The field can be found once the four unknown functions in Eqs. 7-10 have been determined. The functions are determined by the four integral equations:

$$2U_b^i(x) - U_b(x) = \frac{\epsilon_1}{\epsilon_2} \int_{-a}^a G_1(x, b; x', b) DU_b(x') dx', \quad (14)$$

$$U_0(x) = \frac{\epsilon_3}{\epsilon_2} \int_{-a}^a G_3(x, 0; x', 0) DU_b(x') dx', \quad (15)$$

$$\frac{1}{2} U_b(x) = - \int_{-a}^a [G_2(x, b; x', 0) DU_0(x') - U_0(x') \partial_{z'} G_2(x, b; x', z')|_{z \rightarrow 0+}] dx' \\ + \int_{-a}^a [G_2(x, b; x', b) DU_b(x')] dx', \quad (16)$$

$$\frac{1}{2} U_0(x) = - \int_{-a}^a [G_2(x, 0; x', b) DU_b(x') - U_b(x') \partial_{z'} G_2(x, 0; x', z')|_{z \rightarrow b-}] dx' \\ - \int_{-a}^a [G_2(x, 0; x', 0) DU_b(x')] dx', \quad (17)$$

where $|x| < a$, and $U_b^i(x) = \exp[ik_1(x \sin \Theta - b \cos \Theta)]$. A set of the coupled integral equations (14-17) for the four boundary functions can be solved numerically (for details, see¹³) through the matrix equation:

$$\begin{pmatrix} \mathbf{D}^{\text{II}} \mathbf{S}^{\text{III}} - \mathbf{R}^{\text{II}} & \mathbf{S}^{\text{II}} + \frac{1}{2} \mathbf{S}^{\text{I}} \\ \mathbf{S}^{\text{II}} + \frac{1}{2} \mathbf{S}^{\text{III}} & \mathbf{D}^{\text{II}} \mathbf{S}^{\text{I}} - \mathbf{R}^{\text{II}} \end{pmatrix} \begin{pmatrix} DU_0(x) \\ DU_b(x) \end{pmatrix} = \begin{pmatrix} U_b^i(x) \\ 2\mathbf{D}^{\text{II}} U_b^i(x) \end{pmatrix} \quad (18)$$

where

$$R_{kj}^{II} = \frac{i}{2N\gamma_0} \exp(i\gamma_0 b) + \frac{i}{N} \sum_{m=1}^{\infty} \frac{1}{\gamma_m} T_m^{j,k} \exp(i\gamma_m b), \quad (19a)$$

$$D_{kj}^{II} = \frac{1}{2N} \exp(i\gamma_0 b) + \frac{1}{N} \sum_{m=1}^{\infty} T_m^{j,k} \exp(i\gamma_m b), \quad (19b)$$

$$S_{kj}^{II} = \frac{i}{2N\gamma_0} + \frac{i}{N} \sum_{m=1}^{\infty} \frac{1}{\gamma_m} T_m^{j,k}, \quad (19c)$$

$$T_m^{j,k} = \frac{2N}{m\pi} \cos \left[\frac{m\pi(j-1/2)}{N} \right] \cos \left[\frac{m\pi(k-1/2)}{N} \right] \sin \left[\frac{m\pi}{2N} \right]. \quad (20)$$

b. The analytical model and formulae Let us now present an approximate analytical solution of the scattering problem. For a subwavelength slit, the thin-slit condition $2a \ll \lambda$ is a very good approximation. In such a case, it can be easily demonstrated that an accurate solution exists for the above matrix equation in the case of $N = 1$, which is valid at $|z| > 2a/N$ (see, ref.¹³). We have derived the simple formulae for the transmitted electromagnetic field and the transmission coefficient using the thin-slit approximation. After simple calculation using the above equations with $N = 1$, the analytical formulae for the magnetic $\vec{H}(x, z)$ and electric $\vec{E}(x, z)$ fields in region III can be presented as

$$\vec{H}(x, z) = iaH_0^{(1)}(k[x^2 + z^2]^{1/2})(DU_0)_1 \vec{e}_y, \quad (21)$$

$$E_x(x, z) = -a \frac{z}{[x^2 + z^2]^{1/2}} H_1^{(1)}(k[x^2 + z^2]^{1/2})(DU_0)_1, \quad (22)$$

$$E_y(x, z) = 0 \quad (23)$$

and

$$E_z(x, z) = a \frac{x}{[x^2 + z^2]^{1/2}} H_1^{(1)}(k[x^2 + z^2]^{1/2})(DU_0)_1, \quad (24)$$

where

$$(DU_0)_1 = \frac{4}{ik} \frac{\exp(ikb - ikb \cos \theta)}{[\exp(ikb) \cdot (A - ik)]^2 - (A + ik)^2} \quad (25)$$

and

$$A = ia \left[H_0^{(1)}(ka) + \left(\frac{\pi}{2} \right) [\vec{F}_0(ka) H_1^{(1)}(ka) - \vec{F}_1(ka) H_0^{(1)}(ka)] \right]. \quad (26)$$

Here, $H_0^{(1)}(ka)$ and $H_1^{(1)}(ka)$ are the Hankel functions, and $\vec{F}_0(ka)$ and $\vec{F}_1(ka)$ are the Struve functions; for the sake of simplicity, we presented the formulae for the slit placed in vacuum. The transmission coefficient is determined by the time averaged Poynting vector (energy flux) \vec{S} of the electromagnetic field. The vector is calculated as $\vec{S} = (\vec{E} \times \vec{H}^* + \vec{E}^* \times \vec{H})$. The transmission coefficient $T = S_{int}^3$ is given by the normalized flux $S_n^3 = S^3/S^i$ integrated over the slit width $2a$ at the slit exit (region III, $z \rightarrow 0^-$), where $S^3 = S^3(U_3)$ is the z component of the transmitted flux, and S^i is the incident flux along the z direction. For the transmission coefficient we have obtained the following simple analytical formula

$$T(\lambda, a, b) = \frac{a}{k \cos \theta} \cdot [(\text{Re}(DU_0)_1)^2 + (\text{Im}(DU_0)_1)^2]. \quad (27)$$

Notice, that the definition of the transmission coefficient T is equivalent to the more convenient one defined as the integrated transmitted flux divided by the integrated incident flux.

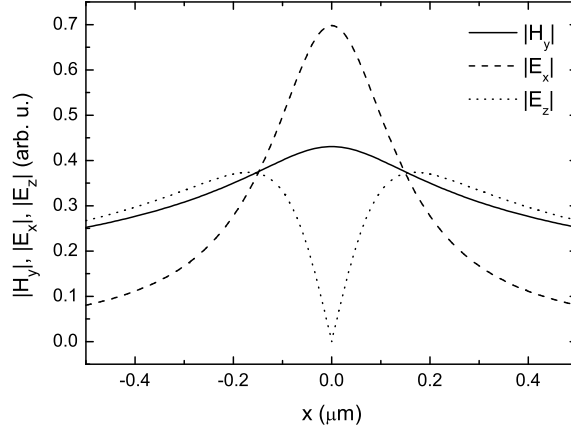


FIG. 2: The near-field distributions $|H_y|$, $|E_x|$ and $|E_z|$ of the transmitted wave with $\lambda = 2500$ nm calculated at $z = -150$ nm for the slit width $2a = 150$ nm and the screen thickness $b = 150$ nm.

III. COMPARISON WITH MODEL BASED ON RAYLEIGH'S FIELD EXPANSION

The analytical formulae (21-27) for the transmitted electromagnetic field and the transmission coefficient have been derived by using the thin-slit ($2a \ll \lambda$) approximation and the Green function formalism for the solution of Maxwell's equations. The main objective of our analysis is to test the accuracy and range of validity of the formulae. We have calculated the magnetic $\vec{H}(x, z)$ and electric $\vec{E}(x, z)$ fields of the transmitted wave for different parameters of the slit. As an example, Fig. 2 shows the near-field ($z = 150$ nm) distributions $|H_y(x, z)|$, $|E_x(x, z)|$ and $|E_z(x, z)|$ calculated by the analytical formulae (21-24) for the slit width $2a = 150$ nm and the screen thickness $b = 150$ nm. The distributions are in agreement with the rigorous numerical computer model¹³. The field components H_y and E_x are collimated to approximately the aperture width $2a$ (see, Fig. 2). Thus, the energy flux S_z of a wave passing through a subwavelength slit can be used to provide a subwavelength image with the optical resolution of about $2a$. We calculated the magnetic $\vec{H}(x, z)$ and electric $\vec{E}(x, z)$ fields of the transmitted wave also in the region ($|z| > 2a/N$, $N = 1$). The calculations showed that the accuracy of the formulae (21-24) decreases with decreasing the value $|z|$.

The transmission of light by the slit is a process that depends on the wavelength. Due to the dispersion, the amplitude of a wave does change under propagation through the slit. This leads to attenuation or amplification of the wave intensity. In our analytical model, the transmission coefficient $T(\lambda, a, b)$ is described by the analytical formula (27). We now check the consistency of the results by comparing the transmission coefficient $T(\lambda)$ calculated by using the semi-analytical model¹ with those obtained by our formula (27).

Analysis of Eq. 27 indicates the slit-wave interaction behavior, which is similar to those of a Fabry-Perot resonator. The minimum thickness of the screen is required to get the waveguide resonance inside the slit at a given wavelength. Figure 3 shows the transmission coefficient (curve A) as a function of the wavelength λ calculated by using the formula (27) for the slit width $2a = 150$ nm and the screen thickness ($b = 150$ nm) smaller than the wavelength λ . The transmission coefficient (curve B) calculated in the study¹ is presented in the figure for comparison. In contrast to the study¹, the transmission (curve A) calculated by our formula exhibits resonance peak, while curve B demonstrates no resonances. In Fig. 3, the screen thickness b has been chosen in such a way as to include one Fabry-Perot resonant wavelength $\lambda_{FP} = 2b$. We notice that the resonance peak is red shifted in comparison with the respective Fabry-Perot wavelength $\lambda_{FP} = 300$ nm. In Fig. 4, the slit includes several Fabry-Perot resonances at the wavelengths $\lambda_{FP} = 2b/n$. Figure 4 shows the transmission (curve A) as a function of the wavelength λ calculated by using the formula (27) for the slit width $2a = 150$ nm and the screen thickness ($b = 1000$ nm) greater than the wavelength. The transmission spectra calculated for the same slit in the study¹ is presented in the figure for the comparison. The transmission (curves A and B) shown in Fig. 4, indicates the slit-wave interaction behavior, which is similar to those of a Fabry-Perot resonator. The transmission resonance peaks, however, have a systematic shift from the Fabry-Perot wavelength $\lambda_{FP} = 2b/n$ ($n=1,2,3,\dots$) towards longer wavelengths. We notice that the resonance wavelengths determined by our formulae are in agreement with the model¹, which solves the wave equations by using the Rayleigh field expansion. The peak heights (curve A), however, are different from the results¹. Our formula

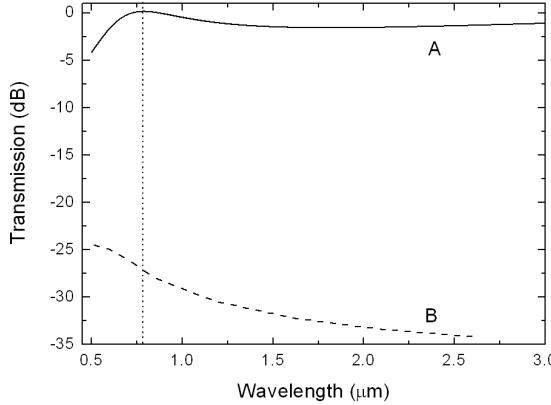


FIG. 3: The transmission (curve A) as a function of the wavelength calculated by using the analytical formula (27) for the slit width $2a = 150$ nm and the screen thickness $b = 150$ nm. The curve B shows the transmission calculated in the study¹. The dotted vertical line corresponds to the resonant wavelength given by the analytical formula.

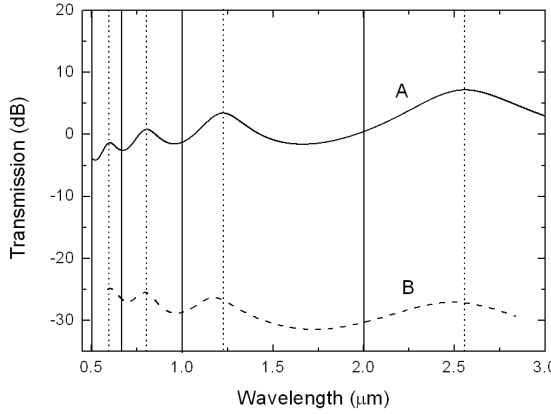


FIG. 4: The transmission (curve A) as a function of the wavelength calculated by using the analytical formula (27) for the slit width $2a = 150$ nm and the screen thickness $b = 1000$ nm. The curve B shows the transmission calculated in the study¹. The dotted vertical lines correspond to the resonant wavelengths given by the analytical formula. The respective Fabry-Perot resonances are indicated by vertical solid lines

(27), predicts the great resonant enhancement of a transmitted wave, while the Rayleigh expansion model¹ indicates attenuation. This indicates the limitations of the model¹.

Analysis of the denominator of the formulae (25-27) shows that the transmission will exhibit the maximum around the Fabry-Perot wavelengths $\lambda_{FP} = 2b/n$ ($n=1,2,3\dots$). The shifts of the resonance wavelengths from the values $\lambda_{FP} = 2b/n$ are caused by the wavelength dependent term in the denominator of Eq. 27 (see, Eqs. 25, 26). The values of the resonant wavelengths and the shifts calculated using the analytical formula (27) are in good agreement with the values calculated using the analytical formula of the study¹. The formula (27), however, shows the great resonant enhancement of a transmitted wave, while the Rayleigh expansion model¹ predicts attenuation. The difference is attributed to the influence of the near-field subwavelength diffraction, which is not considered by the models based on the Rayleigh field expansion. Indeed, the Rayleigh-like expansion models use the two component decomposition $U_1(z) \sim U^i(z) + U^r(z)$ in one dimension, which does not take into account the near-field diffraction. The Green-function model, however, uses the field $U_1(x, z) = U^i(x, z) + U^r(x, z) + U^d(x, z)$, which includes the near-field diffraction field $U^d(x, z)$ in two dimensions.

IV. SUMMARY AND CONCLUSION

We have presented an analytical model of the resonantly enhanced transmission of light through a subwavelength nm-size slit in a thick metal film. The simple formulae for the transmitted electromagnetic fields and the transmission coefficient were derived by using the thin-slit approximation and the Green function formalism for the solution of Maxwell's equations. The resonance wavelengths are in agreement with the semi-analytical model¹, which solves the wave equations by using the Rayleigh field expansion. Our formulae, however, show great resonant enhancement of a transmitted wave, while the Rayleigh expansion model predicts attenuation. The transparent explanation of the difference between the results of the two models was presented. The difference is attributed to the near-field subwavelength diffraction, which is not considered by the models based on the Rayleigh field expansion. We believe that the presented analytical model gains insight into the physics of resonant transmission and localization of light by subwavelength nanoapertures in metal films.

Acknowledgments

This study was supported by the Fifth Framework of the European Commission (Financial support from the EC for shared-cost RTD actions: research and technological development projects, demonstration projects and combined projects. Contract No NG6RD-CT-2001-00602) and in part by the Hungarian Scientific Research Foundation (OTKA, Contract Nos T046811 and M045644) and the Hungarian R&D Office (KPI, Contract No GVOP-3.2.1.-2004-04-0166/3.0).

-
- ¹ Y. Takakura, Phys. Rev. Lett. **86**, 5601 (2001).
² F.Z. Yang, J.R. Sambles, Phys. Rev. Lett. **89**, 063901 (2002).
³ F.J. García-Vidal, L. Martín-Moreno, Phys. Rev. B **66**, 155412 (2002).
⁴ D.A. Thomas, H.P. Hughes, Solid State Commun. **129**, 519 (2004).
⁵ J. Bravo-Abad, L. Martín-Moreno, F.J. García-Vidal, Phys. Rev. E **69**, 026601 (2004).
⁶ J. Lindberg, K. Lindfors, T. Setala, M. Kaivola, A.T. Friberg, Opt. Express **12**, 623 (2004).
⁷ J.R. Suckling, A.P. Hibbins, M.J. Lockyear, T.W. Preist, J.R. Sambles, C.R. Lawrence, Phys. Rev. Lett. **92**, 147401 (2004).
⁸ Y. Xie, A.R. Zakharian, J.V. Moloney, M. Mansuripur, Opt. Express **12**, 6106 (2004).
⁹ S.V. Kukhlevsky, M. Mechler, L. Csapó, K. Janssens, and O. Samek, Phys. Rev. B **70**, 195428 (2004).
¹⁰ C. Liu, C.C. Yan, Y. Lin, H. Chen, Chin. Phys. Lett. **22**, 1784 (2005).
¹¹ F. L. Neerhoff and G. Mur, Appl. Sci. Res. **28**, 73 (1973).
¹² R.F. Harrington and D.T. Auckland, IEEE Trans. Antennas Propag. **AP28**, 616 (1980).
¹³ E. Betzig, A. Harootunian, A. Lewis, and M. Isaacson, Appl. Opt. **25**, 1890 (1986).